

**Holonomy corrected Schwarzschild black hole lensing**A. R. Soares<sup>1,\*</sup>, C. F. S. Pereira<sup>2,†</sup>, R. L. L. Vitória<sup>3,‡</sup> and Erick Melo Rocha<sup>4,5,§</sup><sup>1</sup>*Grupo de Estudos e Pesquisas em Laboratório de Educação matemática, Instituto Federal de Educação Ciência e Tecnologia do Maranhão, Rua Deputado Gastão Vieira, 1000, CEP 65393-000 Buriticupu, Maranhão, Brazil*<sup>2</sup>*Departamento de Física e Química, Universidade Federal do Espírito Santo, Avenida Fernando Ferrari, 514, Goiabeiras, Vitória, Espírito Santo 29060-900, Brazil*<sup>3</sup>*Faculdade de Física, Universidade Federal do Pará, Avenida Augusto Corrêa, Guamá, 66075-110, Belém, Pará, Brazil*<sup>4</sup>*Instituto Federal de Educação Ciência e Tecnologia do Maranhão, Campus Buriticupu, CEP 65393-000, Buriticupu, Maranhão, Brazil*<sup>5</sup>*MUST University Florida, 2220 N Federal Hwy, Boca Raton, Florida 33431, USA* (Received 3 October 2023; accepted 11 November 2023; published 8 December 2023)

In the present work, we theoretically investigate gravitational lensing in the spacetime of a holonomy corrected Schwarzschild black hole. Analytical expressions for the light deflection angle are obtained in both the weak field limit and the strong field limit. Furthermore, we analyze observables, such as relativistic images and magnifications, and compare the results with those expected in a Schwarzschild spacetime. We discuss the possibilities and difficulties of investigating such a solution in practice.

DOI: [10.1103/PhysRevD.108.124024](https://doi.org/10.1103/PhysRevD.108.124024)**I. INTRODUCTION**

It is well known that the limitations presented by Einstein's general relativity in dealing naturally with the problem of geodesic singularity have motivated the search for a broader gravitation theory [1–9]. From this perspective, loop-quantum gravity (LQG) emerges as one of the promising quantum gravity proposals with the objective of “regularizing” gravity [10–12]. LQG is a nonperturbative theory to quantize the spacetime structure; however, it does not present a complete quantum description close to what we currently understand as a singularity. In this sense, one can explore the effects of LQG in low-energy regimes through effective models, that is, models with corrections arising from quantum effects. Recently, in [13,14], the authors obtained a solution of a regular, geodesically complete black hole, resulting from anomaly-free holonomy corrections. Some aspects of this model have already been investigated, such as those linked to quasinormal modes [15,16] and horizon area [17]. In this work, specifically, we theoretically investigate aspects linked to gravitational lensing related to the aforementioned spacetime in order to provide theoretical tools with which can observationally investigate the plausibility of the theory.

Gravitational lensing is a phenomenon resulting from the interaction between light and gravity. When light passes through the gravitational field of a given source, it changes its direction of propagation as a result of this interaction [18,19]. If the light passes through a region very far from the source that generated the gravitational field, the angular deflection is small and we call this regime the weak field limit. Conversely, as the distance between the source and the light decreases, the angular deflection increases. In fact, if the light touches a certain minimum distance, the deflection angle diverges, we call this regime the strong field limit. The first studies of lensing in the strong field limit, in the 1960s, showed that relativistic images are too weak [20,21], in addition, there were no lensing equations suitable for this regime. Because of this, the field of research remained at a standstill in the following decades. In [22], Virbhadra and Ellis presented lensing equations suitable for studying lensing in the strong field regime. Later, Bozza developed a suitable methodology to derive the angular deflection of light in the strong field limit [23], which was later improved by Tsukamoto [24]. Since then, gravitational lensing has been investigated in several contexts involving black holes [25–35], wormholes [36–48], topological defects [49–52], modified theories of gravitation [53–61] and regular black holes [62–65].

Combined with these theoretical developments, recent technological advances, such as the Event Horizon Telescope (EHT) [66–71], have strongly activated the field of lensing research in the strong field limit. The next generation Event Horizon Telescope (ngEHT) [72] is

\*adriano.soares@ifma.edu.br

†carlos.f.pereira@edu.ufes.br

‡ricardo.vitoria@pq.cnpq.br, ricardo-luis91@hotmail.com

§erick.rocha@ifma.edu.br

expected to be able to discriminate between relativistic images and the first and second images. This, among other achievements, presents itself as an important tool for distinguishing between observations predicted by general relativity and other theories of gravity, such as LQG, within the high-energy regime.

Motivated by this stimulating context, in this work, we theoretically explore the observational signature in the gravitational lensing of a solution arising from LQG. We compare the results with those predicted by Schwarzschild spacetime in order to distinguish between the two cases and discuss the results. The work is organized as follows. In Sec. II we present the metric that describes the spacetime and calculate the light deflection in the weak field limit. In Sec. III, we analytically obtain an expression for the light deflection in the strong field limit. In Sec. IV we derive the observables in the strong field limit and compare them with those in the Schwarzschild spacetime. We also discuss the possibilities of experimental verification of the solution. In the Sec. V, we concluded.

## II. SPACETIME AND LIGHT DEFLECTION

The line element metric that describes the holonomy corrected Schwarzschild black hole, in spherical coordinates, is given by [13,14]

$$ds^2 = -\left(1 - \frac{2M}{r}\right) dt^2 + \frac{r}{r-a} \left(1 - \frac{2M}{r}\right)^{-1} dr^2 + r^2(d\theta^2 + \sin^2\theta d\phi^2). \quad (1)$$

In (1), the LQG parameter,  $a$ , is such that  $a < 2M$ . It is a static, spherically symmetric and asymptotically flat spacetime. The spacetime given in (1) has a wormhole-like structure, with  $a$  defining a minimal spacelike hypersurface separating the trapped regular BH interior from the anti-trapped other region. However, we will consider light rays that do not cross the event horizon, characterized by  $r = r_h = 2M$ , i.e., we will address regions where  $r > r_h$ , considering the global structure in the form of a Penrose diagram (see Fig. 1), we will work within region I.

Having established the limits of our investigation, let us derive the equations necessary to study lensing. Using the variational method, the Lagrangian corresponding to the minimum distance in the spacetime described in (1), for  $\theta = \frac{\pi}{2}$ , is given by

$$\mathcal{L} = -\left(1 - \frac{2M}{r}\right) \left(\frac{dt}{d\lambda}\right)^2 + \frac{r}{r-a} \left(1 - \frac{2M}{r}\right)^{-1} \left(\frac{dr}{d\lambda}\right)^2 + r^2 \left(\frac{d\phi}{d\lambda}\right)^2. \quad (2)$$

The corresponding Euler-Lagrange equation for the coordinates  $t$  and  $\phi$  leads to the following conserved quantities

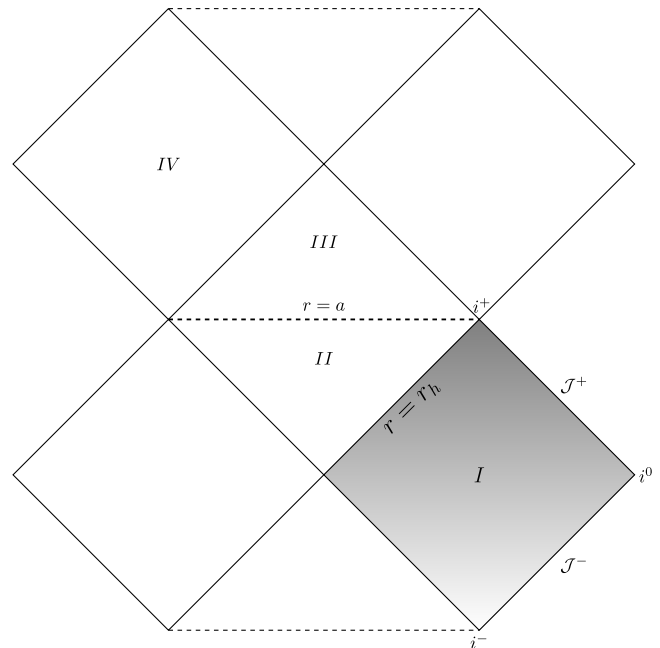


FIG. 1. Penrose diagram. We are analyzing lensing in the shaded region I, beyond to the hypersurface  $r = r_h$ . The other regions correspond to the black hole (II), white hole (III) and another asymptotically flat region (IV) [14].

$$E = \left(1 - \frac{2M}{r}\right) \left(\frac{dt}{d\lambda}\right), \quad (3)$$

and

$$L = r^2 \frac{d\phi}{d\lambda}, \quad (4)$$

which can be understood as energy and angular momentum. Replacing (3) and (4) into (2) and considering null geodesics, where  $\mathcal{L} = 0$ , the (2) leads to

$$\frac{r}{r-a} \left(\frac{dr}{d\lambda}\right)^2 = E^2 - \frac{L^2}{r^2} \left(1 - \frac{2M}{r}\right). \quad (5)$$

Equation (5) can be seen as describing the dynamics of a classical particle of energy  $E$  subject to an effective potential  $V_{\text{eff}} = \frac{L^2}{r^2} \left(1 - \frac{2M}{r}\right)$ . The value of  $r$  for which the orbits are circular is determined by  $\frac{dV_{\text{eff}}(r)}{dr} = 0$ , with this we conclude that the radius photon sphere,  $r_m$ , in the holonomy corrected Schwarzschild BH is given by

$$r_m = 3M, \quad (6)$$

just like in Schwarzschild spacetime.

To analyze the spacetime lensing of a holonomy corrected Schwarzschild BH, let us consider a photon departing from the asymptotically flat region and approaching the BH at a radial distance  $r_0$ , called the turning point, such that

$r_0 > r_m$ . After being deflected by the BH's gravitational field, the photon heads to another asymptotically flat region. At the turning point,  $E = V_{\text{eff}}(r_0)$ , that is,

$$\frac{1}{\beta^2} = \frac{1}{r_0^2} \left(1 - \frac{2M}{r_0}\right), \quad (7)$$

where  $\beta(r_0) = \frac{1}{E}$  is the impact parameter. Replacing (4) in (5), we find

$$\left(\frac{d\phi}{dr}\right) = \left[\left(1 - \frac{a}{r}\right) \left[\frac{r^4}{\beta^2} - r^2 \left(1 - \frac{2M}{r}\right)\right]\right]^{-1/2}. \quad (8)$$

We want to find the change in coordinate  $\phi$ , i.e.,  $\Delta\phi = \phi_- - \phi_+$ . By symmetry, the contributions to  $\Delta\phi$  before and after the turning point are equal, so Eq. (8) leads to

$$\Delta\phi = 2 \int_{r_0}^{\infty} \left[\left(1 - \frac{a}{r}\right) \left[\frac{r^4}{\beta^2} - r^2 \left(1 - \frac{2M}{r}\right)\right]\right]^{-1/2} dr. \quad (9)$$

Let us introduce the following variable change  $u = \frac{1}{r}$ , where we have  $dr = -\frac{du}{u^2}$ . Furthermore,  $u \rightarrow 0$  when  $r \rightarrow \infty$  and  $u \rightarrow u_0$  when  $r \rightarrow r_0$ . Therefore, in terms of  $u$ , (9) becomes

$$\Delta\phi = 2 \int_0^{u_0} \left[\left(1 - au\right) \left[\frac{1}{\beta^2} - u^2(1 - 2Mu)\right]\right]^{-1/2} du. \quad (10)$$

From (7), to (10) becomes

$$\Delta\phi = 2 \int_0^{u_0} \left[(1 - au) \left[u_0^2(1 - 2Mu_0) - u^2(1 - 2Mu)\right]\right]^{-1/2} du. \quad (11)$$

In the weak field approximation, that is, assuming that the photon passes very far from the BH, we can take the approximation  $M \ll 1$  and  $a \ll 1$ . Therefore, up to the second order in  $a$ , a (11) provides the deflection of light  $\alpha = \Delta\phi - \pi$ :

$$\alpha \simeq \frac{4M}{\beta} + \frac{a}{\beta} + \frac{3\pi a^2}{16\beta^2} + \frac{Ma(3\pi - 4)}{4\beta^2}. \quad (12)$$

In Eq. (12), the first term refers to the deflection of a Schwarzschild BH, while the following terms bring a contribution from the holonomic correction. Later, we will study the observational implications of these corrections.

### III. EXPANSION FOR DEFLECTION OF LIGHT IN THE STRONG FIELD LIMIT

In this section, we will obtain the expression for the deflection of light in the strong field limit. To do this, we

will adopt the methodology developed in [23,24]. Making the following variable change

$$z = 1 - \frac{r_0}{r}, \quad (13)$$

the (9) becomes

$$I(r_0) = \int_0^1 \frac{2r_0}{\sqrt{G(z, r_0)}} dz, \quad (14)$$

where

$$G(z, r_0) = \frac{r_0^4}{\beta^2} - \frac{ar_0^3}{\beta^2}(1-z) - r_0^2(1-z)^2 + (2M+a)r_0(1-z)^3 - 2Ma(1-z)^4. \quad (15)$$

Expanding  $G(z, r_0)$  in power series, we obtain

$$G(z, r_0) \simeq \alpha_1(r_0)z + \alpha_2(r_0)z^2, \quad (16)$$

with

$$\alpha_1(r_0) = 6aM - 2ar_0 - 6Mr_0 + 2r_0^2 \quad (17)$$

and

$$\alpha_2(r_0) = 3ar_0 + 6Mr_0 - 12aM - r_0^2. \quad (18)$$

In the strong field limit,  $r_0 \rightarrow r_m = 3M$ , the expansion coefficients are

$$\alpha_1(r_0) \rightarrow \alpha_1(r_m) = 0 \quad (19)$$

and

$$\alpha_2(r_0) \rightarrow \alpha_2(r_m) = 9M^2 - 3aM. \quad (20)$$

This demonstrates that the integral (14), in dominant order, diverges logarithmically in the strong field limit. In order to obtain an expression for the deflection of light in the strong field limit, we will divide (14) into two parts, a divergent part  $I_D(r_0)$  and a regular part  $I_R(r_0)$ , where

$$I_R(r_0) = I(r_0) - I_D(r_0). \quad (21)$$

The divergent part is given by

$$I_D(r_0) = \int_0^1 \frac{2r_0}{\sqrt{\alpha_1(r_0)z + \alpha_2(r_0)z^2}} dz, \quad (22)$$

whose integration provides

$$\begin{aligned}
 I_D(r_0) = & -\frac{4r_0}{\sqrt{\alpha_2(r_0)}} \log\left(\sqrt{\alpha_1(r_0)}\right) \\
 & + \frac{4r_0}{\sqrt{\alpha_2(r_0)}} \log\left(\sqrt{\alpha_2(r_0)}\right) \\
 & + \sqrt{\alpha_1(r_0) + \alpha_2(r_0)}. \quad (23)
 \end{aligned}$$

Now let us expand  $\alpha_1(r_0)$  and  $\beta(r_0)$  close to the radius of the photon sphere. From (17) and (7), we are left with

$$\alpha_1(r_0) \simeq (6M - 2a)(r_0 - 3M) \quad (24)$$

and

$$\beta(r_0) \simeq \sqrt{27M^2} + \sqrt{\frac{3}{4M^2}}(r_0 - 3M)^2. \quad (25)$$

From (24) and (25), we have that

$$\alpha_1(r_0) \simeq 2\sqrt{6}(3M^2 - aM) \sqrt{\left(\frac{\beta}{\sqrt{27M^2}} - 1\right)}. \quad (26)$$

Replacing (26) in (23) and considering the strong field limit, that is,  $r_0 \rightarrow r_m = 3M$ , we get

$$\begin{aligned}
 I_D = & -\sqrt{\frac{3M}{3M-a}} \log\left(\frac{\beta}{3\sqrt{3}M} - 1\right) \\
 & + \sqrt{\frac{3M}{3M-a}} \log(6). \quad (27)
 \end{aligned}$$

The regular part, (21), is given by

$$\begin{aligned}
 I(r_0) = & \int_0^1 \frac{2r_0}{\sqrt{G(z, r_0)}} dz \\
 & - \int_0^1 \frac{2r_0}{\sqrt{\alpha_1(r_0)z + \alpha_2(r_0)z^2}} dz. \quad (28)
 \end{aligned}$$

In the limit  $r_0 \rightarrow r_m = 3M$  and taking into account (15), (16) and (7), (28) leads to

$$\begin{aligned}
 I_R = & \sqrt{\frac{12}{3-2(a/2M)}} \\
 & \times \log\left(\frac{18-12(a/2M)}{6-(a/2M)+3\sqrt{3-2(a/2M)}}\right). \quad (29)
 \end{aligned}$$

Therefore, putting together (29) and (27), we finally find the expansion for the deflection of light in the strong field limit,

$$\begin{aligned}
 \alpha(\beta) = & -\sqrt{\frac{3M}{3M-a}} \log\left(\frac{\beta}{3\sqrt{3}M} - 1\right) \\
 & + \sqrt{\frac{3M}{3M-a}} \log(6) + \sqrt{\frac{12}{3-2(a/2M)}} \\
 & \times \log\left(\frac{18-12(a/2M)}{6-(a/2M)+3\sqrt{3-2(a/2M)}}\right) \\
 & - \pi. \quad (30)
 \end{aligned}$$

One can easily check that when the LQG parameter,  $a$ , tends to zero, the deflection falls into the well-known expression referring to the Schwarzschild spacetime [23]:

$$\alpha(\beta) = -\log\left(\frac{b}{3\sqrt{3}M} - 1\right) + \log(6) + 0.9496 - \pi. \quad (31)$$

In Fig. 2 we plot the light deflection for some values of  $a/2M$ , we see that it is a function that increases with LQG parameter. The solid curve corresponds to the well-known Schwarzschild spacetime case. In Fig. 3 we plot  $\alpha$  as a

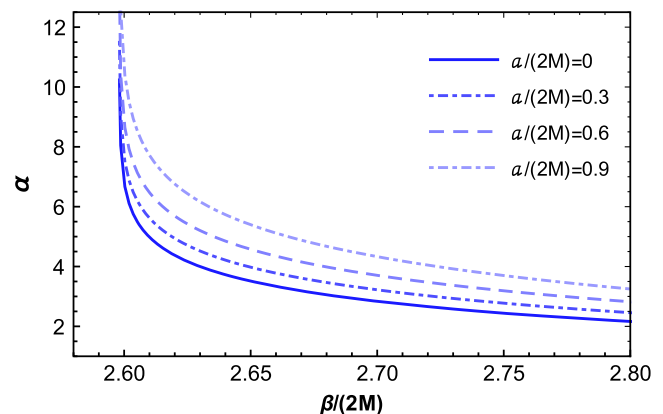


FIG. 2. Light angular deflection as a function of the impact parameter  $\beta/2M$  for various values of the LQG parameter  $a/2M$ .

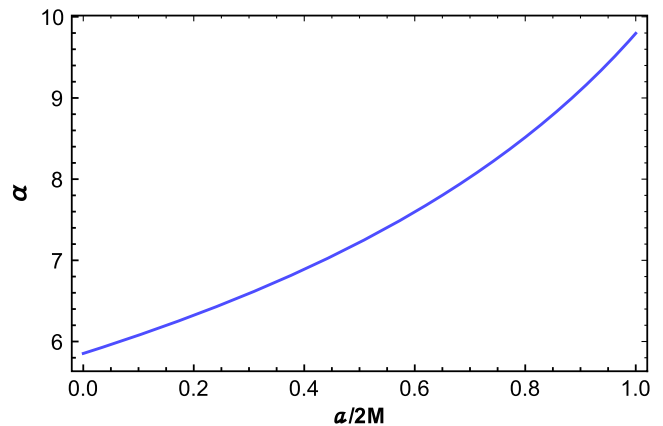


FIG. 3. Light angular deflection as a function of  $a/2M$  for  $\frac{\beta}{2M} = \frac{3\sqrt{3}}{2} + 0.005$ .

function of  $a/2M$  for  $\frac{\beta}{2M} = \frac{3\sqrt{3}}{2} + 0.005$ , that is, we are considering the deflection for a small radial displacement from the critical impact parameter as a function of the LQG parameter. As we can see more clearly, the deflection is a function that increases with the LQG parameter  $a/2M$ . This already indicates that the higher the LQG parameter, the more expressive the discrimination between the deviation of light in comparison to the Schwarzschild spacetime, which really demonstrates the coherence of the results.

#### IV. OBSERVABLES

Now that we have obtained the expressions for the deflection of light in the weak field limit (12) and in the strong field limit (30), let us investigate, through gravitational lensing, what to expect observationally from the LQG spacetime. First, we will briefly review the lens equations in the strong field limit, then we will use them to derive expressions for the observables, with which we can observationally investigate the plausibility of the solution and distinguish it from the Schwarzschild black hole.

The visual profile of the lensing is schematized in Fig. 4. The light that is emitted by the source  $S$  is deflected towards the observed  $O$  by the LQG compact object located in  $L$ . The angular deflection of light is given by  $\alpha$ . The angular positions of the source and image in relation to the optical axis,  $\overline{LO}$ , are given, respectively, by  $\psi$  and  $\theta$ .

As in [22,73], we will admit that the source ( $S$ ) is almost perfectly aligned with the lens ( $L$ ) which is where relativistic images are most expressive. In this case, the lens equation relating the angular positions  $\theta$  and  $\beta$  is given by

$$\psi = \theta - \frac{D_{LS}}{D_{OS}} \Delta\alpha_n, \quad (32)$$

where  $\Delta\alpha_n$  is the least deflection angle of all the loops made by the photons before reaching the observer, that is,  $\Delta\alpha_n = \alpha - 2n\pi$ . In this approximation,

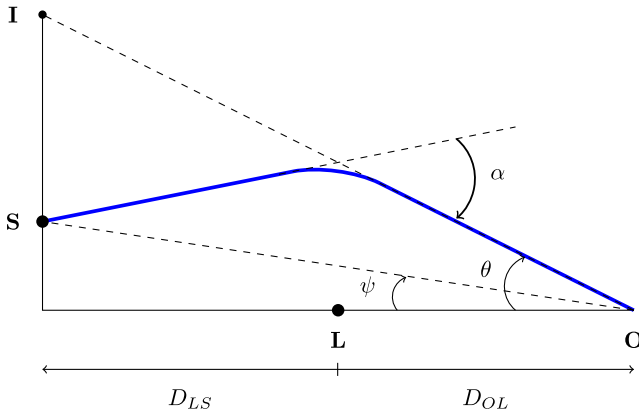


FIG. 4. Light angular deflection diagram.

$$\beta \simeq \theta D_{OL}, \quad (33)$$

so that, for simplicity, we can write the angular deflection (30) as

$$\alpha(\theta) = -\bar{a} \log\left(\frac{\theta D_{OL}}{\beta_c} - 1\right) + \bar{b}, \quad (34)$$

where, compared to (30), we have

$$\bar{a} = \sqrt{\frac{3M}{3M-a}}, \quad (35)$$

$$\begin{aligned} \bar{b} = & \sqrt{\frac{3M}{3M-a}} \log(6) + \sqrt{\frac{12}{3-2(a/2M)}} \\ & \times \log\left(\frac{18-12(a/2M)}{6-(a/2M)+3\sqrt{3-2(a/2M)}}\right) \\ & - \pi, \end{aligned} \quad (36)$$

and

$$\beta_c = 3\sqrt{3}M. \quad (37)$$

What enters the lens equation is  $\Delta\alpha_n$ , to obtain it we expand  $\alpha(\theta)$  close to  $\theta = \theta_n^0$ , where  $\alpha(\theta_n^0) = 2n\pi$ . Thus, we are left with

$$\Delta\alpha_n = \left. \frac{\partial\alpha}{\partial\theta} \right|_{\theta=\theta_n^0} (\theta - \theta_n^0). \quad (38)$$

Evaluating (34) in  $\theta = \theta_n^0$ , we obtain

$$\theta_n^0 = \frac{\beta_c}{D_{OL}} (1 + e_n), \quad \text{where } e_n = e^{\frac{b-2n\pi}{\bar{a}}}. \quad (39)$$

Substituting (34) and (39) into (38), we get

$$\Delta\alpha_n = -\frac{\bar{a}D_{OL}}{\beta_c e_n} (\theta - \theta_n^0). \quad (40)$$

Substituting (40) in the lens equation (32), we obtain the expression for the  $n$ th angular position of the image

$$\theta_n \simeq \theta_n^0 + \frac{\beta_c e_n}{\bar{a}} \frac{D_{OS}}{D_{OL}D_{LS}} (\psi - \theta_n^0). \quad (41)$$

Although the deflection of light preserves surface brightness, gravitational lensing changes the appearance of the source's solid angle. The total flux received by a lensed

image is proportional to the magnification  $\mu_n$ , which is given by  $\mu_n = \left| \frac{\psi}{\theta} \frac{\partial \psi}{\partial \theta} \right|_{\theta_n}^{-1}$ . Then from (32) and (40), we get

$$\mu_n = \frac{e_n(1+e_n)D_{OS}}{\bar{a}\psi} \left( \frac{\beta_c}{D_{OL}} \right)^2. \quad (42)$$

In fact,  $\mu_n$  decreases very quickly with  $n$ , so the brightness of the first image  $\theta_1$  dominates in comparison with other ones. On the other hand, whatever the case, the presence of the factor  $\left(\frac{\beta_c}{D_{OL}}\right)^2$  implies that the magnification will always be small. It should also be noted that at the limit of the source alignment, the lens and observer the magnification diverges, maximizing the possibility of detecting relativistic images.

### A. Observables in the strong field limit

Finally, we have expressed the position of the relativistic images as well as their flows in terms of the expansion coefficients ( $\bar{a}$ ,  $\bar{b}$ , and  $\beta_c$ ). Let us now consider the inverse problem, that is, from observations, determine the expansion coefficients. With this, we can understand the nature of the object that generates the gravitational lens and compare it with the predictions made by modified theories of gravity.

From Eqs. (41) and (39), we have that

$$\theta_\infty = \theta_\infty^0 = \frac{\beta_c}{D_{OL}}. \quad (43)$$

Therefore, we can express the critical impact parameter as

$$\beta_c = D_{OL}\theta_\infty. \quad (44)$$

Let us follow Bozza [23] and assume that only the outermost image  $\theta_1$  is discriminated as a single image while the rest are encapsulated in  $\theta_\infty$ . Therefore, Bozza defined the following observables,

$$s = \theta_1 - \theta_\infty = \theta_\infty e^{\frac{\bar{b}-2\pi}{\bar{a}}}, \quad (45)$$

$$\tilde{r} = \frac{\mu_1}{\sum_{n=2}^{\infty} \mu_n} = e^{\frac{2\pi}{\bar{a}}}. \quad (46)$$

In the expressions above,  $s$  is the angular separation and  $\tilde{r}$  is the relationship between the flow of the first image and the flow of all others. These forms can be inverted to obtain the expansion coefficients. To evaluate the observables, let us consider that the object in question has an estimated mass of  $4.4 \times 10^6 M_\odot$  and is at an approximate distance of  $D_{OL} = 8.5$  Kpc, these data are the same for the black hole at the center of our galaxy [74]. As  $\beta_c = 3\sqrt{3}M$  does not depend on  $a$ , we can calculate it directly. In geometric units, where  $M \rightarrow M \frac{G}{c^2}$ , we will have  $\theta_\infty \simeq 26,5473 \mu$  arcsecs; which is the same as the Schwarzschild case, therefore, it is more promising to investigate the other

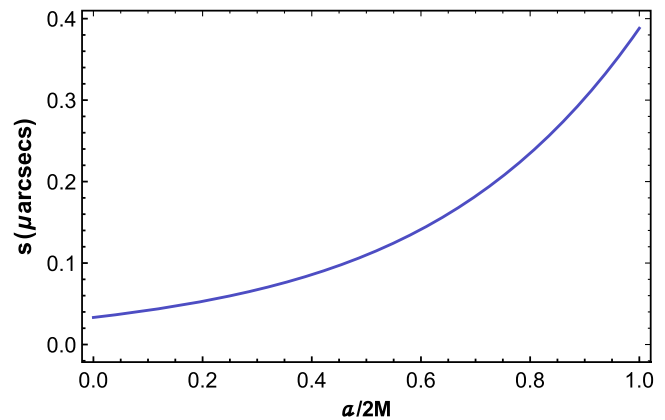


FIG. 5. Angular separation  $s$  as a function of  $a/2M$ .

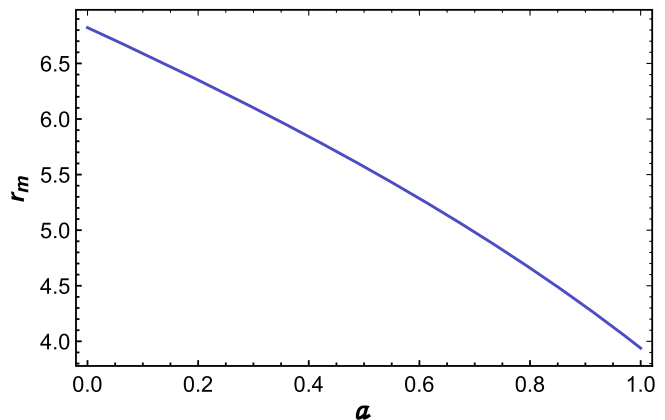


FIG. 6.  $2.5 \log_{10} \tilde{r}$  as a function of  $a/2M$ .

parameters. We plot the behavior of the angular separation in Fig. 5 as a function of  $\frac{a}{2M}$ . In Fig. 6, we plot

$$r_m = 2.5 \log_{10} \tilde{r} \quad (47)$$

in function of  $\frac{a}{2M}$ . As we can see, the angular separation increases with  $a$ , while  $r_m$  decreases. In Table I, we present the observables for some values of the parameter  $\frac{a}{2M}$ , where  $\frac{a}{2M} = 0$  corresponds to the Schwarzschild case. We observe that for  $\frac{a}{2M} \geq 0.6$  the angular separation increases by an order of magnitude compared to the Schwarzschild case. Given the increase in optical resolution of observational projects [72], we hope in the coming decades to have minimum conditions to discriminate different theories of gravitation, however, it is still a great challenge. As we can

TABLE I. Observables.

$a/(2M)$	$s$ ( $\mu$ arcsecs)	$r_m$ (magnitudes)
0	0.0332	6.8218
0.3	0.0673	6.1017
0.6	0.1412	5.2842
0.9	0.3026	4.3145

still see from the graphs and tables, the ratio between the flow of the first and other images decreases, indicating an increase in the magnitude of the other images.

### B. Observables in the weak field limit

The weak field limit corresponds to a very large impact parameter ( $\beta \gg M$ ), so that there are no loops performed by light. In this limit, Eq. (12) gives

$$\alpha \sim \frac{4M + a}{\beta}. \quad (48)$$

In the perfect alignment between the source, the compact object and the observer, we have  $\psi = 0$ , this implies, from Eq. (32), that

$$\theta = \frac{D_{LS}}{D_{OS}} \Delta\alpha_n, \quad (49)$$

with  $\Delta\alpha_n$  given by (48). Therefore, substituting (48) into (49), we find

$$\theta = \theta_E = \sqrt{\frac{D_{LS}(4M + a)}{D_{OS}D_{OL}}}, \quad (50)$$

where  $\theta_E$  is the angular position of the Einstein ring. Beforehand, it is clear that the presence of the LQG parameter,  $a$ , increases the angular position of the Einstein ring. From (33), we can also calculate the radius of the Einstein ring,  $R_E$ , which is given by

$$R_E = D_{OL}\theta_E. \quad (51)$$

Let us now estimate the observables  $R_E$  and  $\theta_E$  taking into account reasonable values for the LQG parameter. As in [48], let us consider the lensing of a bulge star. The following parameters are adopted:  $D_{OS} = 8$  Kpc and  $D_{OL} = 4$  Kpc. Based on these estimates, in the Table II, we present some values of the observables for the presented scenario. We verified that, within the possibilities of the LQG gravity, the present solution presents feasible theoretical possibilities of being detected since the measurements are within the range of observables.

Let us make some observations about the limitation of this work. To calculate the observables, we use the conventional formulation for the lens equation [Eq. (32)]. A general formulation for a spherically symmetric and static

spacetime is given in [75] and improved by Takizawa *et al.* [76], in order to solve the lens equation through iterative methods. In [76], the method is described clearly and in detail, but in order to analyze second-order corrections in holonomy correction, let us give a brief summary of the method here. In the iterative scheme, angles are considered small and expanded in terms of an iterative parameter ( $\epsilon$ ):  $\psi = \epsilon\psi_{(1)}$ ,  $\theta = \sum_{k=1}^{\infty} \epsilon^k \theta_{(k)}$ ,  $\alpha = \sum_{k=1}^{\infty} \epsilon^k \alpha_{(k)}$ . Substituting these expressions into the general lens equation gives the lens equation in all orders. For example, in the leading order [ $\mathcal{O}(\epsilon)$ ], we get the conventional lens equation,

$$\psi_{(1)} = \theta_{(1)} - \frac{D_{LS}}{D_{OS}} \alpha_{(1)}. \quad (52)$$

At second order [ $\mathcal{O}(\epsilon^2)$ ], the general lens equation gives

$$\theta_{(2)} = \frac{D_{LS}}{D_{OS}} \alpha_{(2)}, \quad (53)$$

and so on. Next, we outline the steps that allow us to calculate  $\theta_{(2)}$ . To do so, let us write  $\beta = \epsilon D_{OL} + \epsilon^2 D_{OL} + \mathcal{O}(\epsilon^3)$ , the mass  $M \rightarrow \epsilon^2 M$  and  $a \rightarrow \epsilon^2 a$ . Substituting these values into (12) we obtain

$$\alpha_{(2)} = \frac{3a\pi - 16D_{OL}\theta_{(2)}}{16D_{OL}^2\theta_{(1)}}(a + 4M) - \frac{aM}{D_{OL}^2\theta_{(1)}^2}. \quad (54)$$

Replacing (54) in (53), we find

$$\theta_{(2)} = \frac{3a\pi}{32D_{OL}} - \frac{aM}{2D_{OL}(a + 4M)}. \quad (55)$$

With the expression (55), we estimate the values of  $\theta_{(2)}$  for  $0 < a/2M < 1$ ; in all cases we find that  $\theta_{(2)} \sim 10^{-6}$  arcsecs. This contribution is far below the observational range, which justifies, in the present case, considering the conventional lens equation (leading order in  $\epsilon$ ).

## V. CONCLUSIONS

In this work, we theoretically investigate the gravitational lensing produced by a recently proposed spacetime that is motivated by LQG. We provide analytical expressions for the deflection of light in both the strong field and weak field limits. Furthermore, we carried out a more detailed study of the images generated in the strong field limit, when the light passes very close to the photon sphere. In order to compare our results with those predicted by a Schwarzschild black hole, we modeled the solution with black hole data at the center of our galaxy and calculated the observables. We show that the angular separation increases with the LQG parameter,  $a$ , and, on the other hand, the relativistic images have increased intensity. We emphasize that this distinction between observables,

TABLE II. Einstein radii/angle for bulge lensing.

$\frac{a}{2M}$	$R_E$ (km)	$\theta_E$ (arcsecs)
0	$1.26 \times 10^{12}$	2.11
0.3	$1.35 \times 10^{12}$	2.26
0.6	$1.44 \times 10^{12}$	2.41
0.9	$1.52 \times 10^{12}$	2.54

generated by different models, is crucial for the investigation of gravitational theories beyond general relativity. We further investigated the influence of the LQG parameter on the Einstein ring, concluding that for reasonable values of  $a$ , the radius and angular position of the ring differ significantly from the results predicted by the Schwarzschild solution. We hope that the present work, due to its analytical and numerical results, will contribute,

in due time, to verifying the possibility of corrections to general relativity.

## ACKNOWLEDGMENTS

The authors C. F. S. P. and R. L. L. V. would like to thank CAPES (Coordenação de Aperfeiçoamento de Pessoal de Nível Superior) for financial support.

- 
- [1] R. Penrose, *Phys. Rev. Lett.* **14**, 57 (1965).  
 [2] S. W. Hawking and R. Penrose, *Proc. R. Soc. A* **314**, 529 (1970).  
 [3] E. Berti *et al.*, *Classical Quantum Gravity* **32**, 243001 (2015).  
 [4] T. Clifton, P. G. Ferreira, A. Padilla, and C. Skordis, *Phys. Rep.* **513**, 1 (2012).  
 [5] S. Capozziello and M. De Laurentis, *Phys. Rep.* **509**, 167 (2011).  
 [6] A. De Felice and S. Tsujikawa, *Living Rev. Relativity* **13**, 3 (2010).  
 [7] F. S. N. Lobo, [arXiv:0807.1640](https://arxiv.org/abs/0807.1640).  
 [8] J. Beltran Jimenez, L. Heisenberg, G. J. Olmo, and D. Rubiera-Garcia, *Phys. Rep.* **727**, 1 (2018).  
 [9] S. Nojiri, S. D. Odintsov, and V. K. Oikonomou, *Phys. Rep.* **692**, 1 (2017).  
 [10] C. Rovelli, *Proc. Sci. QGQS2011 (2011) 003* [[arXiv:1102.3660](https://arxiv.org/abs/1102.3660)].  
 [11] A. Ashtekar and E. Bianchi, *Rep. Prog. Phys.* **84**, 042001 (2021).  
 [12] A. Perez, *Rep. Prog. Phys.* **80**, 126901 (2017).  
 [13] A. Alonso-Bardají, *Phys. Lett. B* **829**, 137075 (2022).  
 [14] A. Alonso-Bardají, D. Brizuela, and R. Vera, *Phys. Rev. D* **106**, 024035 (2022).  
 [15] G. Fu, D. Zhang, P. Liu, X. M. Kuang, and J. P. Wu, [arXiv:2301.08421](https://arxiv.org/abs/2301.08421).  
 [16] Zeus S. Moreira, C. D. Lima Haroldo Jr., Luís C. B. Crispino, and Carlos A. R. Herdeiro, *Phys. Rev. D* **107**, 104016 (2023).  
 [17] F. C. Sobrinho, H. A. Borges, I. P. R. Baranov, and S. Carneiro, *Classical Quantum Gravity* **40**, 145003 (2023).  
 [18] A. Einstein, *Science* **84**, 506 (1936).  
 [19] S. Liebes, Jr., *Phys. Rev.* **133**, B835 (1964).  
 [20] C. Darwin, *Proc. R. Soc. A* **249**, 180 (1959); **263**, 39 (1961).  
 [21] R. Atkinson, *Astron. J.* **70**, 517 (1965).  
 [22] K. S. Virbhadra and George F. R. Ellis, *Phys. Rev. D* **62**, 084003 (2000).  
 [23] V. Bozza, *Phys. Rev. D* **66**, 103001 (2002).  
 [24] N. Tsukamoto, *Phys. Rev. D* **95**, 064035 (2017).  
 [25] E. F. Eiroa, G. E. Romero, and D. F. Torres, *Phys. Rev. D* **66**, 024010 (2002).  
 [26] E. F. Eiroa and D. F. Torres, *Phys. Rev. D* **69**, 063004 (2004).  
 [27] N. Tsukamoto and Y. Gong, *Phys. Rev. D* **95**, 064034 (2017).  
 [28] A. B. Aazami, C. R. Keeton, and A. O. Petters, *J. Math. Phys. (N.Y.)* **52**, 102501 (2011).  
 [29] A. B. Aazami, C. R. Keeton, and A. O. Petters, *J. Math. Phys. (N.Y.)* **52**, 092502 (2011).  
 [30] S. Vázquez and E. P. Esteban, *Nuovo Cimento* **119B**, 489 (2004).  
 [31] V. Bozza, F. De Luca, G. Scarpetta, and M. Sereno, *Phys. Rev. D* **72**, 083003 (2005).  
 [32] V. Bozza, F. De Luca, and G. Scarpetta, *Phys. Rev. D* **74**, 063001 (2006).  
 [33] V. Bozza, *Phys. Rev. D* **67**, 103006 (2003).  
 [34] K. S. Virbhadra, *Phys. Rev. D* **106**, 064038 (2022).  
 [35] K. S. Virbhadra, [arXiv:2204.01792](https://arxiv.org/abs/2204.01792).  
 [36] K. Nakajima and H. Asada, *Phys. Rev. D* **85**, 107501 (2012).  
 [37] L. Chetouani and G. Clément, *Gen. Relativ. Gravit.* **16**, 111 (1984).  
 [38] K. K. Nandi, Y. Z. Zhang, and A. V. Zakharov, *Phys. Rev. D* **74**, 024020 (2006).  
 [39] T. K. Dey and S. Sen, *Mod. Phys. Lett. A* **23**, 953 (2008).  
 [40] G. W. Gibbons and M. Vyska, *Classical Quantum Gravity* **29**, 065016 (2012).  
 [41] N. Tsukamoto, T. Harada, and K. Yajima, *Phys. Rev. D* **86**, 104062 (2012).  
 [42] K. K. Nandi, A. A. Potapov, R. N. Izmailov, A. Tamang, and J. C. Evans, *Phys. Rev. D* **93**, 104044 (2016).  
 [43] N. Tsukamoto, *Phys. Rev. D* **95**, 084021 (2017).  
 [44] N. Tsukamoto and T. Harada, *Phys. Rev. D* **95**, 024030 (2017).  
 [45] R. Shaikh, P. Banerjee, S. Paul, and T. Sarkar, *J. Cosmol. Astropart. Phys.* **07** (2019) 028.  
 [46] K. Gao, L. H. Liu, and M. Zhu, *Phys. Dark Universe* **41**, 101254 (2023).  
 [47] T. Cai, Z. Wang, H. Huang, and M. Zhu, *Phys. Rev. D* **108**, 023004 (2023).  
 [48] F. Abe, *Astrophys. J.* **725**, 787 (2010).  
 [49] H. Cheng and J. Man, *Classical Quantum Gravity* **28**, 015001 (2011).  
 [50] M. Sharif and S. Iftikhar, *Adv. High Energy Phys.* **2015**, 854264 (2015).  
 [51] J. Man and H. Cheng, *Phys. Rev. D* **92**, 024004 (2015).  
 [52] H. Cheng and J. Man, *Classical Quantum Gravity* **28**, 015001 (2011).  
 [53] H. Sotani and U. Miyamoto, *Phys. Rev. D* **92**, 044052 (2015).  
 [54] S. W. Wei, K. Yang, and Y. X. Liu, *Eur. Phys. J. C* **75**, 253 (2015); **75**, 331(E) (2015).



- [55] A. Bhadra, *Phys. Rev. D* **67**, 103009 (2003).  
[56] E. F. Eiroa, *Phys. Rev. D* **73**, 043002 (2006).  
[57] K. Sarkar and A. Bhadra, *Classical Quantum Gravity* **23**, 6101 (2006).  
[58] N. Mukherjee and A. S. Majumdar, *Gen. Relativ. Gravit.* **39**, 583 (2007).  
[59] G. N. Gyulchev and S. S. Yazadjiev, *Phys. Rev. D* **75**, 023006 (2007).  
[60] S. Chen and J. Jing, *Phys. Rev. D* **80**, 024036 (2009).  
[61] R. Shaikh and S. Kar, *Phys. Rev. D* **96**, 044037 (2017).  
[62] E. F. Eiroa and C. M. Sendra, *Classical Quantum Gravity* **28**, 085008 (2011).  
[63] E. F. Eiroa and C. M. Sendra, *Phys. Rev. D* **88**, 103007 (2013).  
[64] J. R. Nascimento, A. Y. Petrov, P. J. Porfirio, and A. R. Soares, *Phys. Rev. D* **102**, 044021 (2020).  
[65] S. Ghosh and A. Bhattacharyya, *J. Cosmol. Astropart. Phys.* **11** (2022) 006.  
[66] K. Akiyama *et al.*, *Astrophys. J.* **875**, L1 (2019).  
[67] K. Akiyama *et al.*, *Astrophys. J. Lett.* **875**, L2 (2019).  
[68] K. Akiyama *et al.*, *Astrophys. J. Lett.* **875**, L3 (2019).  
[69] K. Akiyama *et al.*, *Astrophys. J. Lett.* **875**, L4 (2019).  
[70] K. Akiyama *et al.*, *Astrophys. J. Lett.* **875**, L5 (2019).  
[71] K. Akiyama *et al.*, *Astrophys. J. Lett.* **875**, L6 (2019).  
[72] <https://www.ngeht.org/>.  
[73] V. Bozza, S. Capozziello, G. Iovane, and G. Scarpetta, *Gen. Relativ. Gravit.* **33**, 1535 (2001).  
[74] R. Genzel, F. Eisenhauer, and S. Gillessen, *Rev. Mod. Phys.* **82**, 3121 (2010).  
[75] V. Bozza, *Phys. Rev. D* **78**, 103005 (2008).  
[76] K. Takizawa, T. Ono, and H. Asada, *Phys. Rev. D* **102**, 064060 (2020).